Mg-Al yttrian zirconolite in a partially melted sapphirine granulite, Vestfold Hills, East Antarctica

SIMON L. HARLEY

Department of Geology and Geophysics, Grant Institute, Kings Buildings, West Mains Road, Edinburgh, Scotland, EH9 3JW

Abstract

A new compositional variety of zirconolite characterized by high Mg, Al, Y_2O_3 and *REE*, and low Fe is described from a sapphirine granulite xenolith entrained in an intrusive norite body which was emplaced into the late Archaean (2520–2480 Ma) Vestfold Hills high-grade terrain during the early Proterozoic. The zirconolite, and similarly Mg-Al rich perrierite-(Ce), formed as a result of sanidinite facies partial melting of the particularly magnesian and aluminous sapphirine granulite xenolith during its incorporation into the *c.* 1170°C basic magma at *c.* 2240 Ma. The high *REE* compared to Al cations require that a previously unrecognized coupled substitution:

$$REE.REE.(Mg,Fe).Ca_{-2}.Ti_{-1}$$

occurs in this zirconolite. Full chemical analyses are presented for zirconolite and perrierite from this unique occurrence.

KEYWORDS: zirconolite, perrierite-(Ce), granulite, Vestfold Hills.

Introduction

ZIRCONOLITE is a rare Ca-Zr-Ti oxide phase found in some lunar basalts (e.g. Busche *et al.*, 1972) and reported from terrestrial localities, either in various igneous associations such as pyroxenite and ultrabasic cumulates, silica-undersaturated alkaline rocks, carbonatites and kimberlites (Platt *et al.*, 1987; and see Purtscheller and Tessadri, 1985 for a review) or in metacarbonates (Purtscheller and Tessadri, 1985; Gieré, 1986; Williams and Gieré, 1988, in press; Zakrzewski *et al.*, 1992; Gieré and Williams, 1992). A new compositional variety of zirconolite has been identified as an accessory phase in a highly magnesian and aluminous sapphirine-enstatite-spinel granulite xenolith entrained within a post-metamorphic noritic intrusive in the Archaean Vestfold Hills, east Antarctica. The geological occurrence and mineral chemistry of this hitherto unreported zirconolite and perrierite-(Ce) from the same paragenesis are examined in this paper.

Geological setting and mode of occurrence

The Vestfold Hills of east Antarctica comprises an Archaean basement gneiss complex which underwent granulite-facies metamorphic and deformational events between 2501 Ma and 2487 Ma (Black *et al.*, 1991). Orthogneisses, which dominate the terrain, include an earlier suite of mainly tonalitic gneisses whose igneous precursors were emplaced in the interval 2526–2500 Ma (Mossel Gneisses of Collerson *et al.*, 1983) and a younger suite of felsic to intermediate and gabbroic gneisses whose precursors were emplaced between 2500 and 2487 Ma (Crooked Lake Gneisses of Collerson *et al.*, 1983). A suite of metasediments, the Chelnok Paragneiss (formerly Chelnok Supracrustals of Collerson *et al.*, 1983), form about 15% of the terrain. These paragneisses usually comprise garnet quartzites, garnet-sillimanite metapelites and rare calc-silicate.

In the Taynaya Bay region (Fig. 1) a suite of quartz-deficient sapphirine granulites, the

Mineralogical Magazine, June 1994, Vol. 58, pp. 259–269

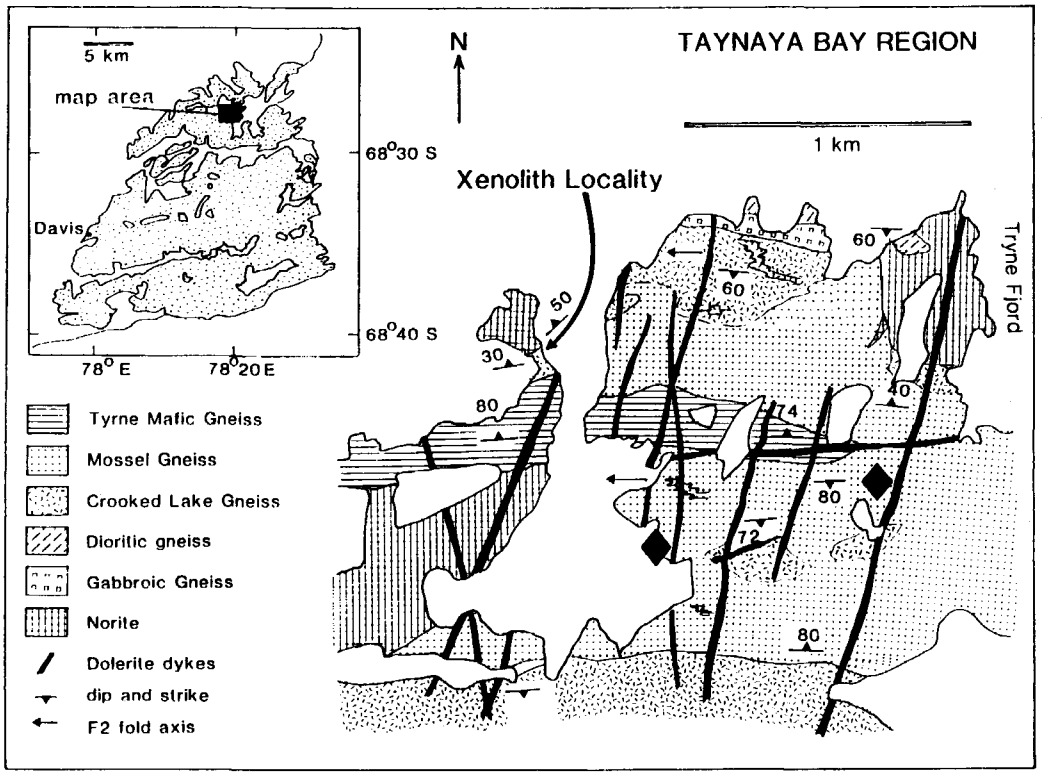

FIG. 1. Location map of the Taynaya Bay area, Vestfold Hills, east Antarctica, showing the general basement geology and outcrops of Taynaya Paragneiss (large diamond symbols) in addition to the site of the zirconolite-bearing Mg-Al sapphirine granulite xenolith. Inset map: position of main map area within the Vestfold Hills.

Taynaya Paragneiss, are recognized (Harley, 1993). These may correlate with the Chelnok Paragneiss found elsewhere in the Vestfold Hills (Harley, 1993), but are distinguished from the latter on the basis of their unusually magnesian and aluminous bulk compositions. The sapphirine granulites, which occur as boudins within Mossel gneisses and xenoliths in the Crooked Lake gneisses, consist of granoblastic mosaics of colourless Mg-sapphirine, enstatite, spinel and minor phlogopite, all with X_{Mg}[100 × Mg/(Mg+Fe)] greater than 90 (Harley, 1993).

A basic ring and dyke complex, the Long Peninsula Norite, intruded the basement gneisses at 2240 Ma (Lanyon *et al.*, 1992), locally entraining fragments of the country rock as xenoliths ranging in diameter from 5–40 cm. The zirconolite reported here occurs dispersed in a 10 × 16 cm sapphirine granulite nodule sampled from a xenolith-rich norite wall zone on Black Island, Taynaya Bay (Fig. 1). This xenolith partially preserves the original textures, mineral assemblages and phase compositions found in sapphirine granulites of the Taynaya Paragneiss cropping out in the basement gneisses outside the norite body and is equivalent to them in terms of bulk composition.

A variety of new textural features attributed to partial melting of the sapphirine granulite xenolith at *c.* 1170°C (Harley and Christy, in press) are superimposed on original granoblastic metamorphic textures involving sapphirine, enstatite and spinel. These features include interstitial-xenomorphic textures involving feldspars pooled between euhedral spinel and titanian enstatite (Fig. 2*a*), titanian-sapphirine euhedra and overgrowths on spinel, platey oikocrysts and books of phlogopite, and resorbed early rutile grains replaced by amoeboid rutile-sapphirine intergrowths. Euhedral zirconolite, monazite and perrierite-(Ce) occur as accessory phases within the areas interpreted from the silicate mineral

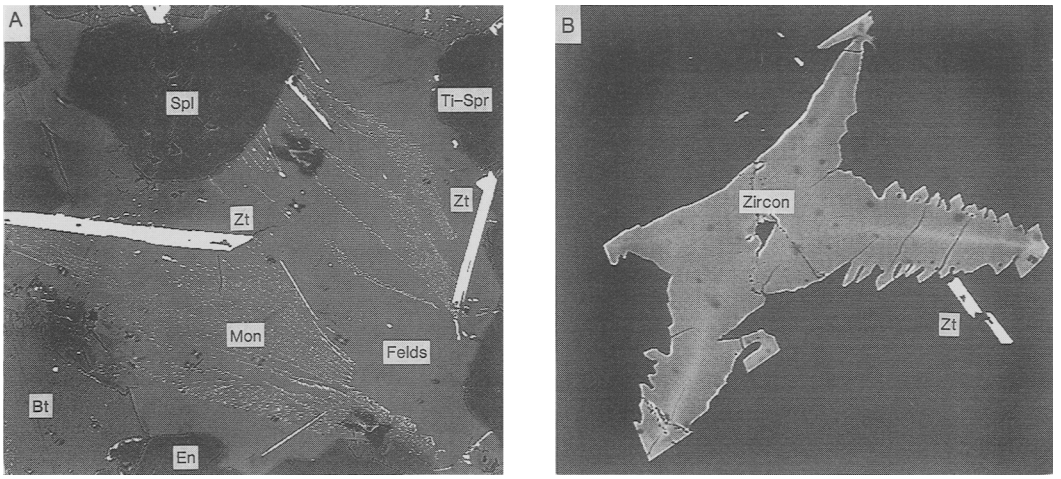

FIG. 2. Textural settings and features of Vestfold Hills zirconolite. (*a*) BEI photomicrograph of a feldspathic pseudomorph (Felds) after a former melt pool. Note subhedral spinel (Spl), enstatite (En) ,and titanian sapphirine (Ti-Spr) growing on spinel in the left of the photograph, and book of biotite (Bt) interstitial to these phases. Zirconolite (Zt) forms bright acicular and platey euhedra growing randomly into the pool or wholly within it. Width of field 0.7 mm. (*b*) BEI photomicrograph of 'stellate' shaped zircon showing growth spikes and a hollow core. The spikes on the crystal limbs have cuspate surfaces in three dimensions. Note bright core and medial rib lines, signifying higher average atomic mass in these areas and consistent with this being a growth form of zircon. Finer bright elongate grains are zirconolites (Zt). Width of field 0.3 mm.

textures to have been melt pools at the time of pyrometamorphism (Fig. 2*a*). Dendritic textures involving monazite and fluid inclusions, and scalloped and hopper- or stellate-shaped zircon grains (Fig. 2*a,b*) are attributed to rapid saturation of the crystallizing melts in trace elements, and may also indicate relatively rapid quenching.

Zirconolite occurs as euhedral platelets, prisms, and acicular grains up to 300 μm long, exclusively contained within the regions where interstitial-xenomorphic and euhedral textures are developed. It is, therefore, a product of the melting and melt crystallization history associated with xenolith entrainment in the norite, and is not a phase produced in the much earlier 2501–2487 Ma granulite metamorphism which affected the Taynaya Paragneiss and other basement gneisses. Red-brown to orange-red zirconolite grows as radiating plates from spinel into the feldspathic areas or occurs as isolated grains in similar pseudomorphs after previous melt patches (Fig. 2*a*). Pink titanian sapphirine (X_{Mg} = 98, TiO_2 = 1.2 wt.%) commonly overgrows both spinel and the zirconolite flakes on spinel (X_{Mg} = 96), indicating that the zirconolite was not the last phase to crystallize but rather was relatively early. The Ti-saturated and silica-poor partial melt is inferred on the basis of the textures and mineral chemistries to have formed through reactions such as:

phlogopite + rutile + enstatite = spinel + liquid

The melting reactions, conditions of melting and cooling history of this Mg–Al granulite xenolith are discussed in Harley and Christy (in press). It is emphasized that zirconolite has not been observed in the sapphirine granulites of the Taynaya Paragneiss, from which the xenolith has been derived; rutile is the only titanian phase present in those precursor rocks.

Analytical Methods

Zirconolite and perrierite-(Ce) have been analysed using a 4 spectrometer Cameca Camebax electron microprobe at the University of Edinburgh under operating conditions of 20 kV and 20 nA probe current. Minerals, oxides and pure metals were used as standards. Full WDS spectral searches were run for each spectrometer to check for the presence of all possible elements and assess peak overlaps. Analyses were made for the following elements: Mg, Al, Si, Zr, Ca, Ti, Y, La, Ce, Pr, Nd, Sm, Dy, Gd, Er, Yb, Hf, U, Th and Fe in all cases,

TABLE 1. Chemical compositions of zirconolites and perrierite-(Ce)

	Zirconolite									Perrierite -(Ce)
	Vestfolds			Kilda	Lunar	Oetzd	Malawi	Koberg	Adam	Vest
	1	2	3							1
SiO_2	0.10	0.11	0.12	0.10	1.08	0.06	0.07	0.34	<0.05	19.66
TiO_2	32.50	32.95	32.91	29.03	26.90	35.52	27.20	27.40	33.50	17.42
Al_2O_3	2.50	2.73	2.74	0.09	1.14	0.98	0.89	0.30	0.91	7.22
MnO	-	-	-	<0.10	-	0.01	0.28	0.85	0.20	-
FeO	0.84	0.81	0.88	8.26	6.50	3.12	7.96	6.20	2.10	0.31
MgO	2.50	2.65	2.65	0.06	0.58	0.30	0.13	0.42	1.50	2.74
ZnO	-	-	-	-	-	-	-	0.55	-	-
CaO	4.68	4.23	4.62	4.05	4.60	13.39	8.08	7.67	9.80	4.34
ZrO_2	34.34	34.17	34.96	31.33	40.70	35.35	28.80	29.22	30.90	1.07
Y_2O_3	8.21	9.09	8.79	8.11	7.30	2.10	3.23	4.64	1.13	1.35
La_2O_3	0.23	0.23	0.24	0.52	-	-	0.53	0.17	0.23	8.95
Ce_2O_3	2.45	1.87	1.99	2.83	2.11	0.56	2.54	1.80	1.70	22.08
Pr_2O_3	0.58	0.44	0.45	0.63	-	-	0.49	0.36	0.40	2.12
Nd_2O_3	3.27	2.69	2.96	4.66	3.30	0.04	3.98	3.08	1.90	8.94
Sm_2O_3	1.37	1.17	1.30	1.33	-	0.17	0.76	1.15	0.50	1.04
Eu_2O_3	-	-	-	0.29	-	-	0.33	-	-	-
Gd_2O_3	1.79	1.78	1.78	1.63	1.92	0.41	0.86	1.31	0.39	0.54
Dy_2O_3	1.69	1.87	1.70	1.83	1.61	0.34	0.75	0.96	0.31	0.28
Er_2O_3	0.75	0.88	0.77	0.96	-	-	0.35	0.44	<0.17	0.16
Yb_2O_3	0.39	0.55	0.39	0.87	-	-	0.39	0.37	<0.18	0.16
HfO_2	0.65	0.70	0.67	0.92	0.47	0.69	0.44	0.79	0.50	0.13
ThO_2	0.61	0.56	0.44	0.45	0.46	0.39	1.62	1.69	6.40	0.45
UO_2	0.28	0.52	0.36	0.21	0.21	0.02	0.57	1.19	5.60	0.12
Nb_2O_5	0.14	0	-	1.29	0.40	5.94	8.30	2.82	2.20	0
Ta_2O_5	0.02	0	-	0.16	-	0.25	0.69	0.15	<0.27	0
P_2O_5	-	-	-	-	-	-	-	-	-	1.03
BaO	-	-	-	-	-	-	0.06	-	-	-
WO_3	-	-	-	-	-	-	-	0.44	<0.30	-
PbO	-	-	-	<0.10	0.23	0.11	-	0.26	<0.10	-
Cr_2O_3	-	-	-	-	0.44	-	-	-	-	-
Total	99.89	100.0	100.72	99.51	99.95	99.74	99.07	94.42	100.40	100.01
O	7	7	7	7	7	7	7	7	7	22
Ca	0.317	0.285	0.309	0.292	0.320	0.859	0.573	0.574	0.670	0.881
Y	0.276	0.304	0.292	0.290	0.252	0.067	0.114	0.173	0.040	0.136
La	0.005	0.005	0.006	0.013	-	-	0.013	0.004	0	0.626
Ce	0.057	0.043	0.045	0.070	0.050	0.012	0.062	0.046	0.040	1.532
Pr	0.013	0.010	0.010	0.016	-	-	0.012	0.009	0.010	0.146
Nd	0.074	0.060	0.066	0.112	0.077	0.001	0.094	0.077	0.040	0.605
Sm	0.031	0.025	0.028	0.031	-	0.003	0.017	0.028	0.010	0.068
Eu	-	-	-	0.007	-	-	0.007	-	-	-
Gd	0.037	0.037	0.037	0.086	0.041	0.008	0.019	0.030	0.010	0.034
Dy	0.035	0.038	0.034	0.040	0.034	0.007	0.016	0.022	0.010	0.017
Er	0.015	0.017	0.015	0.020	-	-	0.007	0.010	0	0.010
Yb	0.007	0.011	0.007	0.018	-	-	0.008	0.008	0	0.009
Th	0.008	0.008	0.006	0.006	0.007	0.005	0.024	0.027	0.090	0.019
U	0.004	0.007	0.005	0.003	0.003	-	0.014	0.019	0.080	0.005
Pb	-	-	-	-	0.004	0.002	-	0.005	0	0
sum A	0.879	0.850	0.860	0.954	0.788	0.964	0.980	1.032	1.000	4.079

TABLE 1. Contd.

	Zirconolite									Perrierite -(Ce)
	Vestfolds			Kilda	Lunar	Oetzd	Malawi	Koberg	Adam	Vest
	1	2	3							1
Zr	1.059	1.048	1.063	1.027	1.290	1.032	0.928	0.996	0.970	0.099
Hf	0.011	0.012	0.011	0.018	0.009	0.012	0.008	0.016	0.010	0.007
sum B	1.070	1.060	1.074	1.045	1.299	1.044	0.936	1.012	0.980	
Si	0.006	0.007	0.007	-	0.070	0.004	-	0.024	0	3.726
Ti	1.546	1.559	1.544	1.467	1.315	1.599	1.353	1.440	1.620	2.483
Al	0.186	0.202	0.201	0.007	0.087	0.069	0.069	0.025	0.070	1.613
Mn	-	-	-	-	-	-	0.016	0.050	0.010	0
Fe	0.044	0.043	0.046	0.464	0.353	0.156	0.440	0.362	0.110	0.049
Mg	0.236	0.250	0.248	0.006	0.056	0.027	0.013	0.044	0.140	0.779
Nb	0.007	0	0	0.039	0.012	0.161	0.247	0.089	0.060	0
Ta	0	0	0	0.003		0.004	0.011	0	0	0
W	-	-	-	-	-	-	-	0.008	0	-
Zn	-	-	-	-	-	-	-	0.028	-	-
Cr	-	-	-	-	0.023	-	-	-	-	-
P	-	-	-	-	-	-	-	-	-	0.165
Sum C	2.025	2.061	2.046	1.986	1.916	2.020	2.149	2.070	2.010	8.930
Total	3.977	3.971	3.981	3.895	4.003	4.028	4.065	4.114	3.990	13.009
X_{Mg}	84.3	85.3	84.4	1.3	13.7	14.8	2.9	10.8	56.0	94.1
A/AFM	39.9	40.8	40.6	1.5	17.5	27.4	11.7	5.8	21.9	66.1

Sources of data: St. Kilda (Kilda): Fowler and Williams (1986); Lunar: Busche *et al.* (1972)
Oetzdal (Oetzd): Purtscheller and Tessardi (1985); Malawi: Platt *et al.* (1987)
Koberg: Zakrzewski *et al.* (1992); Adamello (Adam): Gieré and Williams (1992)

and additionally for Cr, V, Ta, Ho, Nb, Mn, Na, P and K on selected grains. No correction of Mg for overlap with U-$M\alpha$ and Th-$M\alpha$ has been made as the latter elements have very low abundances. Er was measured on its $L\beta$ peak to avoid overlaps with lighter *REE*. Similarly, Pr and Gd in perrierite-(Ce) were measured on their $L\beta$ peaks to minimize overlap with La-$L\alpha$ and Ce-$L\alpha$ peaks respectively. Representative analyses of zirconolite and perrierite-(Ce) are presented along with relevant literature examples of zirconolite in Table 1.

Zirconolite mineral chemistry

Zirconolite has general formula $AB_xC_{(3-x)}O_7$ based on the additive component $CaZrTi_2O_7$ (Bayliss *et al.*, 1989). Ca in the 8-fold *A* site is replaceable by *REE*, Y, Th, U, Sr, Ba and Pb. Zirconium in the 7-coordinated *B* site can be replaced by Hf and Ti; and Ti in the *C* sites (two 6-fold and one 5-fold sites) may be replaced by Zr, Nb, Fe, Mg, Mn, Al, Si, Ta, W and Zn (Mazzi and Munno, 1983; Purtscheller and Tessadri, 1985; Platt *et al.*, 1987). As a consequence there are a number of simple and coupled exchange vectors possible, and it is very difficult to represent the subtleties of zirconolite chemistry in single triangular diagrams. The major substitutions and chemical variations in the Vestfold Hills zirconolite will be described below and compared to other terrestrial and lunar zirconolites in subsequent sections.

Twenty four analyses obtained on five zirconolite grains indicate that chemical zoning in the Vestfold Hills zirconolite is not significant, and that any heterogeneity is limited to minor complementary variations between Ca and Y_2O_3 + REE_2O_3 on the *A* site. The lack of chemical heterogeneity distinguishes this zirconolite from those recently reported occurring in metacarbonates (Zakrzewski *et al.*, 1992; Gieré & Williams, 1992), which are strongly zoned in several elements. Concentrations of Cr, V, Mn, Na and

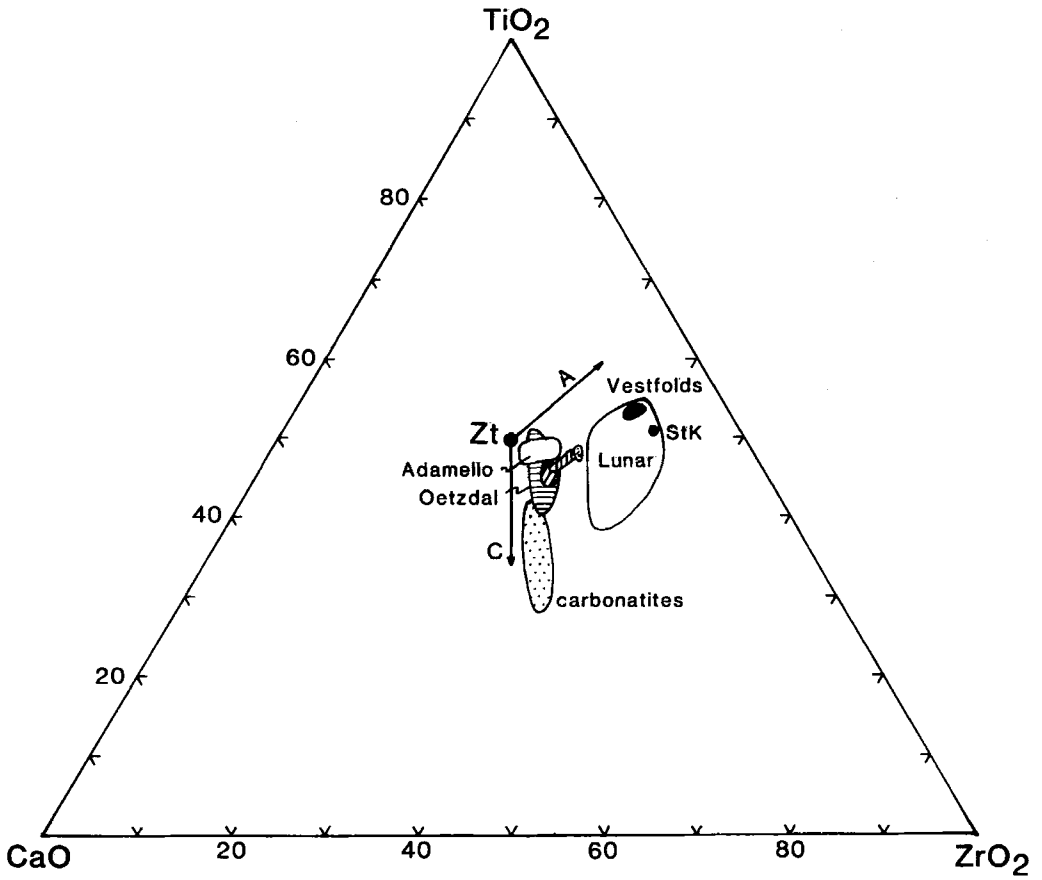

FIG. 3. $CaO-TiO_2-ZrO_2$ diagram showing the compositions of natural zirconolites. Substitution vectors A and C from zirconolite (Zt) are explained in the text. StK is the Saint Kilda zirconolite (Harding *et al.*, 1982). Data for Oetzdal, Lunar, pyroxenite (diagonal ruled area) and carbonatite samples after Purtscheller and Tessardi (1985); Adamello zirconolite from Gieré & Williams (1992); Malawi (vertical ruled field) from Platt *et al.* (1987); Koberg (small stippled field) from Zakrzewski *et al.* (1992).

K are low and near detection limits, while Pb and W have not been detected in the full spectral scan undertaken prior to quantitative analysis.

The principal chemical features of zirconolites can be considered using the Ca–Ti–Zr diagram of Fig. 3, which groups together the three Ti sites (*C*-sites). In this compositional space, end-member zirconolite should plot at the 1:1:2 position, labelled Zt. Most natural examples diverge from this point to lower Ca along the control line 'A' as the *A* site is partially filled with *REE* or U and Th, and along the control line 'C' as Ti is replaced by Nb, Ta, Fe, Mg and Al. The Vestfold Hills zirconolite plots well away from the ideal composition and towards the Ti–Zr side of the diagram. As U and Th are very low, the *A*-site constitution is marked by very high Y and *RE*E (8–9 wt.% Y_2O_3 and 12–13 wt.% total REE_2O_3). Calcium is correspondingly low (4% CaO) and similar to some lunar zirconolites (Busche *et al.*, 1972; see Table 1). The closest equivalent terrestrial example in terms of Ca-content is that from a pegmatite from St. Kilda (Harding *et al.*, 1982), however even this differs in containing high Fe and Nb, negligible Mg and Al, significant U + Th, and higher total Y_2O_3 + REE_2O_3 than the Vestfold Hills zirconolite (Fowler and Williams, 1986).

The coexisting phases enstatite + spinel + phlogopite + sapphirine define a magnesian and aluminous paragenesis and bulk composition unique for zirconolite occurrence and strongly

controls the unique C- or Ti-site chemistry of this zirconolite, which is very poor in Fe relative to Al and Mg. Ti-site occupancies of the Vestfold Hills zirconolite are compared with other terrestrial samples in the AFM plot of Fig. 4. Total Al+Fe+Mg cations are in the upper end of the range defined by most zirconolites (0.4 to 0.55 cations Al+Fe+Mg per formula unit). The Vestfold Hills zirconolite defines a distinctive population with very high X_{Mg} (85) and high A/AFM, even compared with the relatively magnesian (X_{Mg} = 52–64) zirconolites described from clinohumite marbles in the Adamello contact aureole by Gieré and Williams (1992). In addition, Nb (and Ta) abundances are uniformly very low to negligible (< 0.2 wt.%) compared with almost all other reported zirconolites, which range from 0.4 wt.% to 8.3 wt.% in Nb_2O_5. For example, the complexly zoned zirconolites reported by Gieré and Williams (1992) contain much higher Nb_2O_5 (0.43–2.2 wt.%).

The Vestfold Hills zirconolite is also characterized by low Hf and total Hf+Zr cations greater than 1.0. Silicon is negligible and the other oxide totals approximate 100%, consistent with a lack of metamictization, which usually enhances Si contents and leads to a decrease in total oxides due to water entrapment (Platt *et al.*, 1987).

Chondrite normalized *REE* patterns for the Vestfold Hills and other selected terrestrial zirconolites are presented in Fig. 5. *LREE* depletion and enrichment in the middle *REE* (Sm, Gd) is a typical feature of all zirconolites. The Vestfold Hills zirconolites have total *REE* similar to that from the St. Kilda gabbro pegmatite occurrence (Fowler and Williams, 1986) but show a broad *MREE* hump rather than the pivoting about normalized maxima in Nd

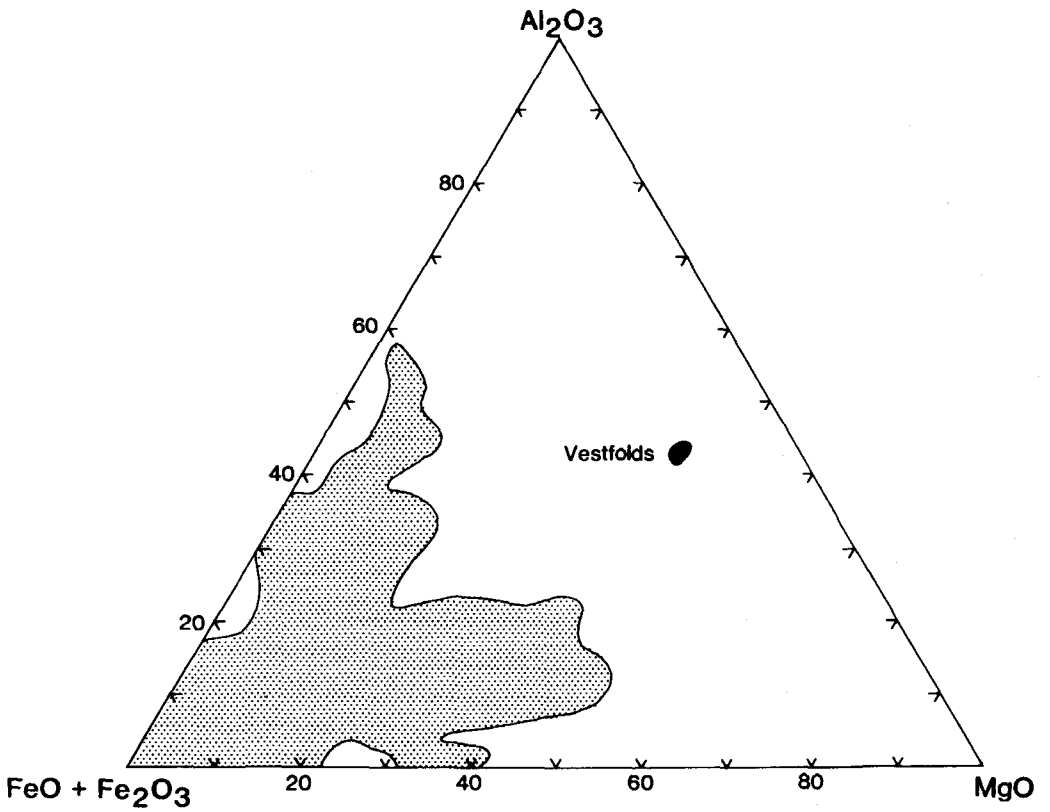

FIG. 4. Al_2O_3–FeO+Fe_2O_3–MgO (AFM) cation plot for zirconolite *C*-sites, demonstrating the uniquely high X_{Mg} and A/AFM of the Vestfold Hills zirconolite compared with all other natural samples. Field of all other natural zirconolites (stippled area, 233 analyses) is based on the data compilation of Williams and Gieré (in press).

or Sm that is apparent in some other examples (Platt *et al.*, 1987).

Perrierite-(Ce)

The *REE*-Fe-Ti silicate phase perrierite-(Ce), with general formula $A_4BC_4Si_4O_{22}$, is usually found as an accessory mineral in peralkaline igneous rocks and pegmatites. The *A*-site may be occupied by *REE*, Th, Ca, Na, K and Sr; the *B*-site by Fe^{2+}, Mg, Mn and Ca; and the *C*-sites by Ti, Fe^{3+}, Fe^{2+}, Mg, Mn and Al (Ito, 1967; Ito and Arem, 1971; Calvo and Faggiani, 1974). Three grains (15 × 40 μm) of perrierite-(Ce) have been identified within feldspathic pseudomorphs after melt pools or stringers in the Vestfold Hills xenolith. Like the zirconolite, the perrierite-(Ce) is compositionally distinct from other reported occurrences (e.g. Segalstad and Larsen, 1978) in its very high Mg and Al contents (MgO + Al_2O_3 = 10 wt.%) coupled with very low Fe and Nb (Table 1) which give rise to high X_{Mg} and A/AFM values (94 and 66 respectively). From the analysis given in Table 1 it is apparent that some Ca probably occurs in the *B*-site (0.079 cations), and that some Si is replaced by Al in the tetrahedral sites. The *REE* composition of this perrierite-(Ce) (Fig. 6) is, however, similar to perrierites and chevkinites from syenites (Segalstad and Larsen, 1978; Platt *et al.*, 1987).

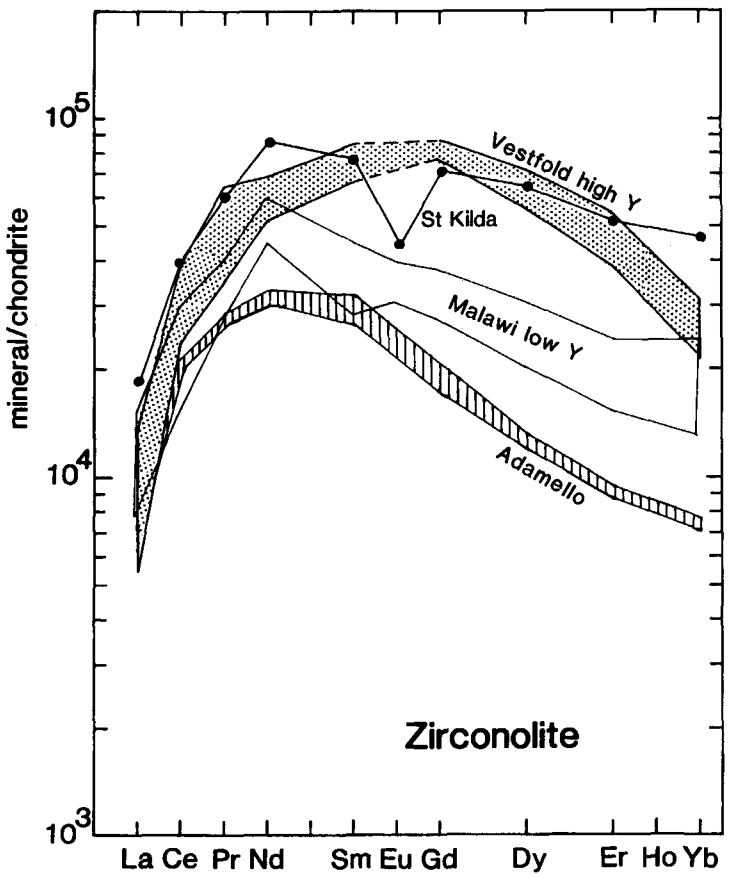

FIG. 5. Chondrite-normalised *REE* plot of the high-Y Vestfold Hills zirconolite analyses (24 analyses, stippled field). Low-Y, high-Nb zirconolites from Malawi syenites (Platt *et al.*, 1987), high-Y zirconolites from Adamello contact aureole marbles (Gieré and Williams, 1992), and high Y + *REE* zirconolites from the Kt Kilda gabbro pegmatite (Fowler and Williams, 1986) are shown for comparison. Chondrite values from Sun and McDonough (1989) used to normalise the Vestfold and St. Kilda data.

As only trace amounts of perrierite-(Ce) have been found in several thin-sections of 88/37 it has not been possible to extract the mineral for X-ray diffraction to confirm it as perrierite rather than its dimorph, chevkinite. Ito (1967) and Segalstad and Larsen (1978) have distinguished chevkinite from perrierite on the basis of average the ionic radius of cations in the *A* and *B*+*C* sites. The Vestfold Hills phase plots well inside the perrierite field as determined by Ito (1967), with average *A* and *B*+*C*-site cation radii of 0.108 and 0.062 nm respectively, and is therefore considered to be perrierite rather than chevkinite.

Discussion and conclusions

Zirconolite cation exchange vectors and high REE+Y. The unique combination of high $Y_2O_3 + REE_2O_3$, high Al+Mg+Fe, and low U+Th and Nb+Ta in the Vestfold Hills zirconolite has important implications for potential coupled substitutions in natural zirconolites. Based on chemical analyses of extensively zoned zirconolites formed at *c.* 500°C, Gieré and Williams (1992) have proposed the following as important coupled substitutions:

(1) (Th,U).(Mg,Fe).Ca_{-1}.Ti_{-1}
(2) *REE*.Al.Ca_{-1}.Ti_{-1}
(3) *REE*.Fe^{2+}.(Nb,Ta).Ca_{-1}.Ti_{-2}
(4) Hf.Zr_{-1}

In the present case the substitutions (1),(3) and (4) are negligible because of the low measured U+Th, Nb+Ta and Hf respectively. However, substitution (2) cannot by itself explain the chemistry of this zirconolite, which has *REE*+Y > Al+Mg+Fe, Mg+Fe > Al, and total

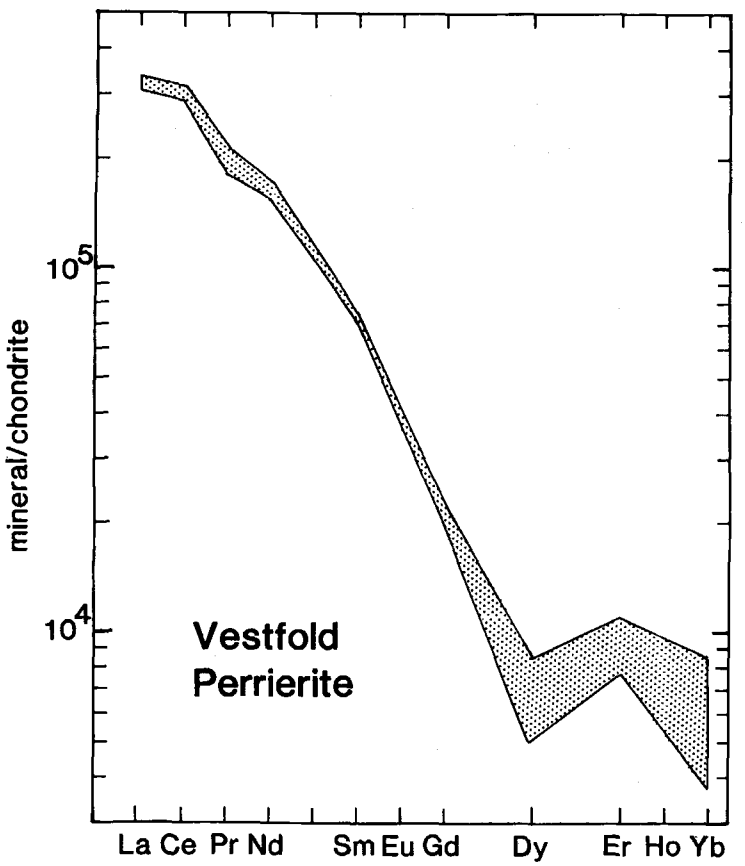

FIG. 6. Chondrite-normalised *REE* plot of perrierite-(Ce) analyses from the Vestfold Hills xenolith (3 analyses, stippled field).

apparent *A*-site occupancy significantly less than 1. The imbalance between *REE*+Y and Al requires that substitutions other than (2) are responsible for much of the *REE* content of this zirconolite. Making the assumption that Zr + Hf in the *B*-site should total 1.0, then some Zr has to be redistributed into the *C*-sites through a $ZrTi_{-1}$ substitution (e.g. 0.07 cations Zr in analysis 1 of Table 1). Adding the requirement that total cations in the *C*-sites should equal 2.0, and assuming that all Fe is divalent, it is apparent that some elements have to be distributed back into the *A*-site (0.095 and 0.120 cations in analyses 1 and 2). It is considered that Mg enters the 8-coordinated *A*-site via the simple exchange $MgCa_{-1}$ in this case. The *REE*+Y cations remaining after allocations to the substitutions (2) and (3) above can then be accounted for through the complex coupled exchange: $REE.REE.(Mg,Fe).Ca_{-2}.Ti_{-1}$ in which the substitution of one Ti by divalent Mg and Fe in the *C*-sites is accommodated by replacement of two Ca by *REE*+Y in the *A*-site. This important coupled substitution, not recognized from previous studies of zirconolites from other localities (Purtscheller and Tessardi, 1985; Platt *et al.*, 1987; Zakrzewski *et al.*, 1992; Gieré and Williams, 1992), is responsible for 58–63% of the total *REE*+Y content of the Vestfold Hills zirconolite.

Conditions of zirconolite formation. The geological occurrence of zirconolite and perrierite-(Ce) reported here is unique. As noted in earlier sections, sapphirine granulites within the felsic granulite basement in the Vestfold Hills have not been observed to host either of these minerals. The formation of zirconolite and perrierite-(Ce) has only occurred through the coincidence of an appropriate bulk composition (bulk X_{Mg} = 98.5) with a low silica content being accidentally entrained and partially melted in a high-temperature intrusive. Partial melting under sanidinite facies conditions caused the instability of primary metamorphic rutile, and allowed solution of significant amounts of zirconium and titanium in the melts, as also indicated by the growth of highly titanian (0.9–1.4 wt.% TiO_2) sapphirine and enstatite in the former melt pools (Harley and Christy, in press). The Mg- and Al-enriched compositions of the Vestfold Hills zirconolite and perrierite-(Ce) are controlled by the unusually magnesian and aluminous nature of the bulk rock. X_{Mg} values of the coexisting phases spinel, sapphirine and enstatite are 98, 98.5 and 99 respectively (Harley and Christy, in press), so that this zirconolite is the least magnesian phase involved in the melting and melt crystallization history despite its high X_{Mg}. This relationship is consistent with Fe–Mg partitioning observed between zirconolite and coexisting silicates in other occurrences. The consistent chemical relations between the Vestfold Hills zirconolite and coexisting silicates, coupled with its exclusive occurrence in feldspathic areas pseudomorphing former melt patches, indicate that the zirconolite formed as an equilibrium phase at 1100–1170°C and 3–4 kbar, the conditions determined on the basis of silicate phase equilibria for partial melting in the xenolith (Harley and Christy, in press).

Acknowledgements

The zirconolite-bearing xenolith was collected on the 1987–88 Australian National Antarctic Research Expedition (ANARE). The support provided by the Australian Antarctic Division and ASAC project grant DV/05/88 is gratefully acknowledged. S. Kearns is thanked for assistance with microprobe analysis. C. T. Williams is thanked for a helpful review and access to an unpublished data compilation by Williams and Gieré (in press).

References

Bayliss, P., Mazzi, F., Munno, R. and White, T. J. (1989) *Mineral. Mag.* **53**, 565–9.

Black, L. P., Kinny, P. K., Sheraton, J. W. and Delor, C. P. (1991) *Precamb. Res.*, **50**, 283–310.

Busche, F. D., Prinz, M., Keil, K. and Kurat, G. (1972) *Earth Planet. Sci. Lett.*, **14**, 313–21.

Calvo, C. and Faggiani, R. (1974) *Amer. Mineral.*, **59**, 1277–85.

Collerson, K. D., Reid, E., Millar, D. and McCulloch, M. T. (1983) *Antarctic Earth Science* (eds. Oliver, R. L., James, P. R., and Jago, J. B.), 77–84.

Fowler, M. B. and Williams, C. T. (1986) *Mineral. Mag.*, **50**, 326–8.

Gieré, R. (1986) *Contrib. Mineral. Petrol.*, **93**, 459–70.

Gieré, R. and Williams, C. T. (1992) *Contrib. Mineral. Petrol.*, **112**, 83–100.

Harding, R. R., Merriman, R. J., and Nancarrow, P. H. A. (1982) *Mineral. Mag.*, **46**, 445–8.

Harley, S. L. (1993) Sapphirine granulites from the Vestfold Hills, East Antarctica: geochemical and metamorphic evolution. *Antarctic Sci.*, **5**, 389–402.

Harley, S. L. and Christy, A. (in press) Titanian 2:2:1 sapphirine in a partially melted aluminous granulite xenolith, Vestfold Hills, East Antarctica *Eur. J. Mineral.*

Ito, J. (1967) *Amer. Mineral.*, **52**, 1094–104.

Ito, J. and Arem, J. E. (1971) *Amer. Mineral.*, **56**, 307–19

Lanyon, R., Black, L. P. and Seitz, H-M. (1992). U–Pb dating of a mafic dyke swarm within the Vestfold Hills, East Antarctica. *Structural and metamorphic studies in high-grade metamorphic terrains*, Abstracts Volume, University of Melbourne.

Mazzi, F. and Munno, R. (1983) *Amer. Mineral.*, **68**, 262–76.

Platt, R. G., Wall, F., Williams, C. T. and Woolley, A. R. (1987) *Mineral. Mag.*, **51**, 253–63.

Purtscheller, F. and Tessardi, R. (1985) *Mineral. Mag.*, **49**, 523–9.

Segalstad, T. V., and Larsen, A. O. (1978) *Amer. Mineral.*, **63**, 499–505.

Sun, S-S. and McDonough, W. F. (1989) *Geol. Soc. Lond. Spec. Publ.* **42**, 313–45.

Williams, C. T. and Gieré, R. (1988) *Schweiz. Mineral. Petr. Mitt.*, **68**, 133–140.

Williams, C. T. and Gieré, R. (submitted) Zirconolite: a review of localities worldwide, and a compilation of its chemical compositions. *Bull. British Mus. Nat. Hist. (Geol)* (submitted 1993)

Zakrzewski, M. A., Lustenhouwer, W. J., Nugteren, H. J. and Williams, C. T. (1992) *Mineral. Mag.*, **56**, 27–35.

[*Manuscript received 18 March 1993: revised 14 September 1993*]